INL/EXT-07-13252

Heterogeneous Transmutation Sodium Fast Reactor

S. Bays

September 2007

The INL is a U.S. Department of Energy National Laboratory
operated by Battelle Energy Alliance

INL/EXT-07-13252

Heterogeneous Transmutation Sodium Fast Reactor

S. Bays

September 2007

Idaho National Laboratory
Idaho Falls, Idaho 83415

Prepared for the
U.S. Department of Energy
Office of Nuclear Energy
Under DOE Idaho Operations Office
Contract DE-AC07-05ID14517

Heterogeneous Transmutation Sodium Fast Reactor

INL/EXT-07-13252

September 2007

Approved by

S. Bays, Principal Author	Date
Mehdi Asgari, Peer Reviewer	Date
David W. Nigg, Department Manager	Date

ABSTRACT

The threshold-fission (fertile) nature of Am-241 is used to destroy this minor actinide by capitalizing upon neutron capture instead of fission within a sodium fast reactor. This neutron-capture and its subsequent decay chain leads to the breeding of even neutron number plutonium isotopes. A slightly moderated target design is proposed for breeding plutonium in an axial blanket located above the active "fast reactor" driver fuel region. A parametric study on the core height and fuel pin diameter-to-pitch ratio is used to explore the reactor and fuel cycle aspects of this design. This study resulted in two core geometries (non-flattened and flattened). Both of these designs demonstrated a high capacity for removing americium from the fuel cycle. A reactivity coefficient analysis revealed that this heterogeneous design will have comparable safety aspects to a homogeneous reactor of comparable size. A mass balance analysis revealed that the heterogeneous design may reduce the number of fast reactors needed to close the current once-through light water reactor fuel cycle.

DISCLAIMER

ACKNOWLEDGEMENTS

The author would like thank Daniel Wessol and Steve Herring (INL) for their initial guidance of this work and for their ongoing technical support. The author would also like to thank Steven Piet, Mitch Meyer and Mehdi Asgari (INL) for their guidance and encouragement. Other contributors deserving thanks are Massimo Salvatores (CEA) and Roald Wigeland (INL) for sharing their experience base with the author.

CONTENTS

FIGURES

TABLES

GLOSSARY, ACRONYMS, AND ABBREVIATIONS

ABR	Advanced Burner Reactor
Am&Cm	Americium and Curium Elemental Grouping
BOEC	Beginning of Equilibrium Cycle
BOL	Beginning of Life
dpa	Displacements per Atom
ENDF	Evaluated Nuclear Data File
EOEC	End of Equilibrium Cycle
EOL	End of Live
EPR	Evolutionary Pressure Reactor
FFTF	Fast Flux Test Facility
HT-SFR	Heterogeneous Transmutation Sodium Fast Reactor
LHGR	Linear Heat Generation Rate
MA	Minor Actinide
MOX	Mixed Oxide
Np&Pu	Neptunium and Plutonium Elemental Grouping
PWR	Pressurized Water Reactor
REBUS	Reactor Burnup System
SFR	Sodium Fast Reactor
SNF	Spent Nuclear Fuel
S-PRISM	Super Power Reactor Innovative Small Module
TRU	Transuranic
UOX	Uranium Oxide

1. Introduction

Generally, for low conversion ratio sodium fast reactors (SFR) with high minor actinide loaded fuels, there is a tradeoff between the optimal Doppler and void coefficients and the attainable minor actinide destruction efficiency. The two most basic SFR feedback mechanisms are the Doppler feedback provided by fertile uranium in the fuel and blankets; and the increase in axial neutron streaming that occurs during coolant voiding. A low conversion ratio can be attained by decreasing the parasitic capture while increasing leakage [1]. .

The tradeoff stems from the fact that the mechanisms commonly used to remove neutrons from the reactor during transients as a passive control mechanism also remove them to some unavoidable extent in steady state operation [2]. For example, enhancing axial streaming with a pancake geometry or a reduced fuel pin diameter makes the void coefficient more negative. But, the increased overall leakage reduces the available excess reactivity. Alternatively, increasing fertile U-238 increases resonance capture and makes the Doppler coefficient more negative. However, this produces further transuranics (TRU) from captures in the same resonances that provide the beneficial feedback. In both cases, more fissile plutonium is required to compensate for reactivity lost. The added plutonium and reduction of fertile material increases the reactor cycle reactivity swing.

The primary rationale for a low conversion ratio is the destruction of plutonium and possibly other undesired transuranics in the fuel cycle. For the current Light Water Reactor (LWR) fuel cycle, these "other" undesired transuranics are the Spent Nuclear Fuel (SNF) Minor Actinides (MA). This is because of the MA concentration of Np-237 and Am-241 within SNF which are the space limiting isotopes to its repository storage. These isotopes have an even neutron number, which gives them longer half lives compared to the odd isotopes of their respective elements. The even number of neutrons also tends to cause these isotopes to have a threshold fission barrier, on the order of 1 MeV. Therefore, this component of TRU is difficult destroyed by fission because most of the neutron flux spectrum in a SFR falls below this 1 MeV threshold. Conversely, neutron capture in these "fertile" minor actinides leads to the generation of the even plutonium isotopes: Pu-238 and Pu-242. Though these plutonium isotopes still have an even neutron number, they are more fissionable than the starting minor actinides in the fast neutron spectrum. These even plutonium isotopes have very little fissile value in thermal reactors but have a significantly larger worth in fast reactors. Therefore, to increase the minor actinide destruction rate while mitigating the negative attributes of a low conversion ratio, it is desirable to first transmute them into plutonium via neutron capture.

Transmuted even-isotope plutonium breeding can be accomplished with a thermalizing flux trap within the SFR. The goal of such a trap is to recover the fast neutrons leaked from the SFR and moderate them to a softer spectrum before irradiating a minor actinide rich target. Because enhanced axial leakage can be achieved with a flattened geometry, the targets are located in an axial blanket residing above a pancake active driver core. Because this core design is both spatially and spectrally heterogeneous, it is dubbed as a Heterogeneous Transmutation Sodium Fast Reactor (HT-SFR).

2. Description of Work

For this work, a parametric study is conducted on the effects of core flattening and heavy metal fuel content on the transmutation performance of the axial targets. Also evaluated is the: cycle length, excess reactivity, and "total core" Doppler coefficient and sodium void worth as a function of this parameter set. All these factors are related to axial leakage and parasitic capture. However, the plutonium generation in the axial targets creates an additional feedback within the fuel cycle that is also a

function of reactor and fuel geometry. Therefore, the purpose of the parametric study is to evaluate the tradeoff between core performance factors and the maximum minor actinide destruction rate.

The target's height and composition are held constant for all points in the parametric evaluation. The targets comprise a 20 cm tall axial blanket placed between the plenum and driver core of the 1000 MWth Advanced Burner Reactor (ABR) design proposed by Hoffman et al. [3]. The lateral core layout is assumed to be identical to the ABR case with a conversion ratio (CR) of 0.5 as shown in Figure 1. Starting with the ABR reference height of 101.6 cm, the active driver core height was varied to 51.6 cm in 10 cm increments. For each one of these active core heights, the range of pin diameter-to-pitch ratios shown in Table 1 was evaluated. The core average volumetric power density was held constant for each height reduction. This was done to give an equally comparable power density, depletion rate and cycle length for each height.

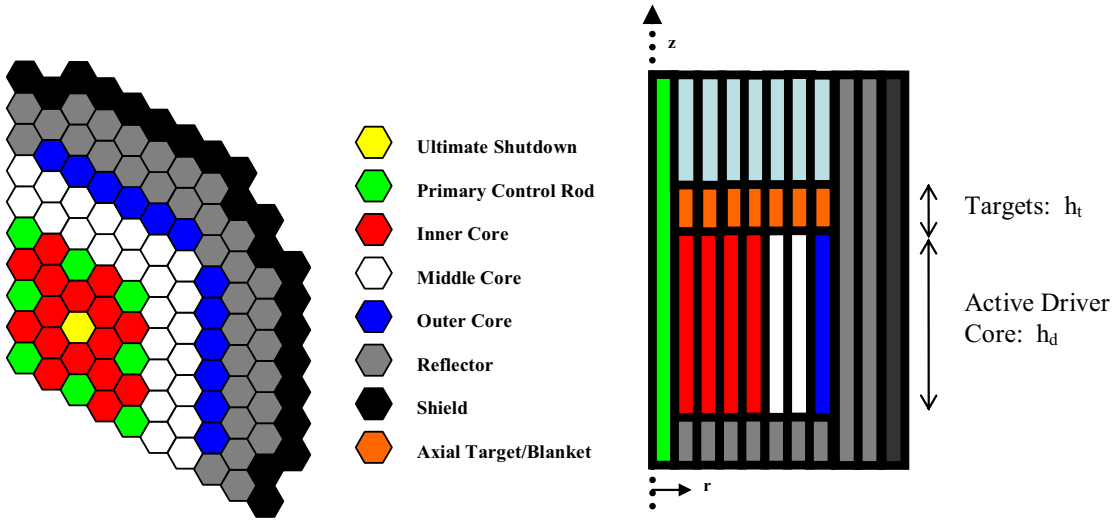

Figure 1: HT-SFR radial and r-z profiles (not an exact scale)

Next, the ABR (CR=0.5) reference radial core design from Figure 1 was evaluated for each increment in pin diameter-to-pitch ratio. These homogeneous reference cases provide the constraining reactor performance parameters for down-selecting to a practical core height and pin diameter.

Table 1: Reference fuel assembly design for varying height-to-diameter ratio.

	p/d=1.1	p/d=1.176	p/d=1.293	p/d=1.357
Fuel assembly pitch: cm	16.142	16.142	16.142	16.142
pins per assembly	271	271	324	540
Fuel Assembly Volume Fraction				
Fuel	34.27%	29.30%	22.08%	17.40%
Bond	11.42%	9.77%	7.36%	5.81%
Structure	25.73%	25.68%	26.41%	29.15%
Coolant	28.79%	35.25%	44.15%	47.60%

Finally, a core height and pin diameter that gives the highest transmutation efficiency while at the same time ensuring reactivity coefficients within the boundaries of the homogeneous reference was

selected. Using this core height and pin diameter combination, additional driver assemblies were added to the core until the HT-SFR thermal power output was 1000 MWth as it is for the ABR design. This gives the HT-SFR a commercial scale by roughly equating the overall core volume. This new flattened and scaled up core design shares similar fuel cycle and reactor performance attributes as the core with the smaller radius from the parametric study. This is attributed to similar axial leakage properties due to the height reduction.

3. Reactor Design and Fuel Cycle

Target fuel rodlets are placed adjacent to $ZrH_{1.6}$ dilution rods in an axial blanket configuration above the driver fuel. A zirconium metallic fuel alloy is assumed for both driver and target rods. Zirconium hydride was selected as the moderator for its high thermal conductivity and melting temperature. A hydrogen-to-zirconium stoichiometric ratio of 1.6 was selected to get the zirconium hydride delta phase which retains a stable composition for temperatures below 1000°C [4]. These rods are collocated within the same fuel pin and share the same plenum space with the driver fuel rods below them. The ratio of target to $ZrH_{1.6}$ containing fuel pins is five to one. Therefore, for a typical hexagonal SFR fuel assembly, 226 of the 271 fuel pins contain targets and 45 contain $ZrH_{1.6}$ above the driver fuel rods.

The accompanying fuel management strategy allows the targets and driver fuel to be discharged and recycled together in the same pyroprocessor batch. After pyroprocessing the mixed target and driver TRU stream supplies fabrication of fresh driver fuel. Fresh targets are fabricated from the americium and curium component of SNF. This americium and curium stream is provided by the UREX+3 separations process. The UREX+3 neptunium and plutonium stream provides the external fissile feed to the driver fuel as well as the targets. Some plutonium is supplied to the targets to minimize the power swing as a result of Pu-238 and Pu-239 generation during the irradiation. As seen in Figure 2, the SNF americium and curium is irradiated only once in targets before it rejoins the neptunium and plutonium in the driver. Therefore, sufficient americium must be destroyed in the targets such that the unburned americium is less than 5 w/o of the heavy metal in the driver. This ensures that the heterogeneous reactor's physics and fuel performance are comparable with the equivalent homogeneous ABR design [5].

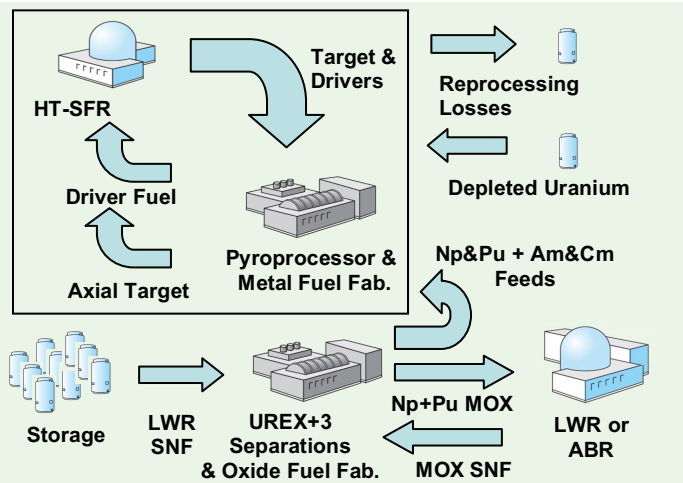

Figure 2: Two-Tier Fuel Cycle Scenario using HT-SFRs to service minor actinides

Similar to the ABR, the active driver fuel has no radial blankets and uses three enrichment zones to flatten the radial power profile across the core [1,6-7]. The driver fuel composition is a TRU/U/10Zr (by

weight) alloy. The ratio of middle and outer core enrichments to that of the inner core is: 1.25 and 1.50 respectively. The target fuel fixed composition is 10Np&Pu/10Am&Cm/40U/40Zr. Some of the UREX+3 separated Np&Pu stream (i.e external feed) is diverted from the active driver fuel supply to the targets. None of the pyroprocessed plutonium is used to refuel the targets. This is mainly because the choice of pyroprocessing does not readily allow for elemental separation. This also allows the higher mass actinides of curium and californium that were generated during the target irradiation to be diluted over a larger fuel inventory. This dilution is intended to reduce the intensity of radiation fields and hence shielding requirements to fuel fabrication workers dealing with recycled material. The target composition was selected for it's similarity to the "uranium-free" AFC-1B tests irradiated at Idaho National Laboratory [8].

4. Calculation Method

The Argonne National Lab fast reactor codes MC^2-2, DIF3D and REBUS are used for the reactor physics and fuel cycle calculations [9]. The MC^2-2 code was used to generate a 33 group cross section set for each enrichment zone, the axial blanket zone and reflectors and shields. Starting with an ultra-fine group ENDF-V/B cross section library, MC^2-2 created a collapsed cross section set by performing a zero dimensional infinite dilution critical buckling search using the extended P1 method [10]. This zero-dimensional approach does not account for spatial shielding effects between the various core regions but for fast reactor calculations is generally sufficient due to the long neutron mean free path. The fast flux is almost entirely in the unresolved resonance range, thus making unresolved energy shielding and the unresolved resonance treatment the dominating effects in the group collapsing. MC^2-2 also performs a resolved resonance broadening treatment at user defined material and fuel temperatures. These cross sections are then used in a criticality calculation performed by DIF3D.

The DIF3D diffusion code was used to solve the multi-group steady state neutron diffusion equation using a hexagonal-z nodal coordinate system [11]. In the nodal discretization, each hexagonal node in the lateral direction represents a fuel assembly. Because the mean free path is on the dimensional level of the fuel assembly, the individual fuel rods are homogenized across this hexagon.

REBUS uses DIF3D to perform a criticality search for the uncontrolled excess reactivity at each time step in its fuel depletion algorithm. Once the criticality search is completed, the fluxes from DIF3D are used in an exponential matrix to carry out the fuel depletion, transmutation and decay of the fuel isotopic vector within the time step. This algorithm assumes that regional fluxes do not change significantly over this time step. REBUS also performs the in-core fuel management and out-of-core cooling, reprocessing and re-fabricating for each reactor cycle. For the HT-SFR, REBUS's equilibrium cycle search option was used to carry out the fuel management steps depicted inside the boxed off portion of Figure 2. These operations were carried out until the excess reactivity and equilibrium cycle length was found. A maximum fuel burnup of 18 a/o after 6 reactor cycles (seven cycles for the outer core) was used to constrain the search procedure for the equilibrium cycle length.

Since REBUS only deals with the closed portion of the fuel cycle, the externally supplied UREX+3 feed is made sufficient to subsidize the pyroprocessor with enough heavy metal to constitute the next batch of fresh fuel. The isotopic vector for the UREX+3 feed was set constant to represent SNF discharged from a pressurized water reactor after a 51 MWD/kg irradiation and cooled for five years. Once this equilibrium was attained, the Beginning of Equilibrium Cycle (BOEC) total core void and Doppler coefficients were calculated. The total core void worth was attained by taking the BOEC number densities from each isotope in each axial and radial region from the REBUS output file into a new DIF3D (no depletion) input file. The number density for sodium for each region was reduced by the coolant volume fraction leaving only the bond sodium in the fuel rod gap with the coolant sodium voided. The sodium fraction was also reduced for the corresponding MC^2-2 calculation.

The Doppler coefficient was calculated in a similar procedure without the change in sodium number density. Instead a new MC^2-2 calculation was performed with all cross sections broadened at a temperature 100 K greater than that for the REBUS calculation. Then a new DIF3D calculation was performed with the BOEC number densities unchanged from the REBUS output file.

5. Target Transmutation Physics

The repository space benefit stems primarilly from the removal of americium from the fuel cycle. This is because the repository's waste emplacement drift spacing is limited by the maximum rock temperature at the midpoint between them. The drift temperature is principally a function of the decay heat produced by Am-241 in the SNF [12]. Because of its long half-life, radiotoxicity, high solubility and low sorption in Yucca Mountain tuffs, Np-237 is the principal environmental concern to the biosphere if water does come into contact with the SNF. Because, Np-237 is the alpha decay product of Am-241, americium destruction in targets also minimizes the Np-237 accumulation in the repository.

Am-241 and Np-237 have an even neutron number and thus the binding energy contribution of an absorbed neutron is not sufficient to overcome the critical energy required for fission. In fact, the addition of a neutron to an odd-neutron nucleus (fissile isotope) to form an even-neutron compound nucleus gives a binding energy change that is about 1 MeV greater than for changing an even-neutron nucleus into an odd-neutron compound nucleus. This explains the fission threshold at 1 MeV for the long lived minor actinides Np-237 and Am-241. A neutron capture in Np-237 generates the fissile Np-238 nucleus. However, Np-238 beta decays into Pu-238 with a short 2.117 day half-life. A neutron capture in Am-241 produces the fissile Am-242,242^{m} isotopes. The yield fraction to the ground state is estimated to be approximately 80% in the fast spectrum. This Am-242 ground state beta decays into Cm-242 with a branching ratio of 83%. The other 17% of Am-242 electron captures to become Pu-242. Cm-242 decays into Pu-238 with a 163 day half-life.

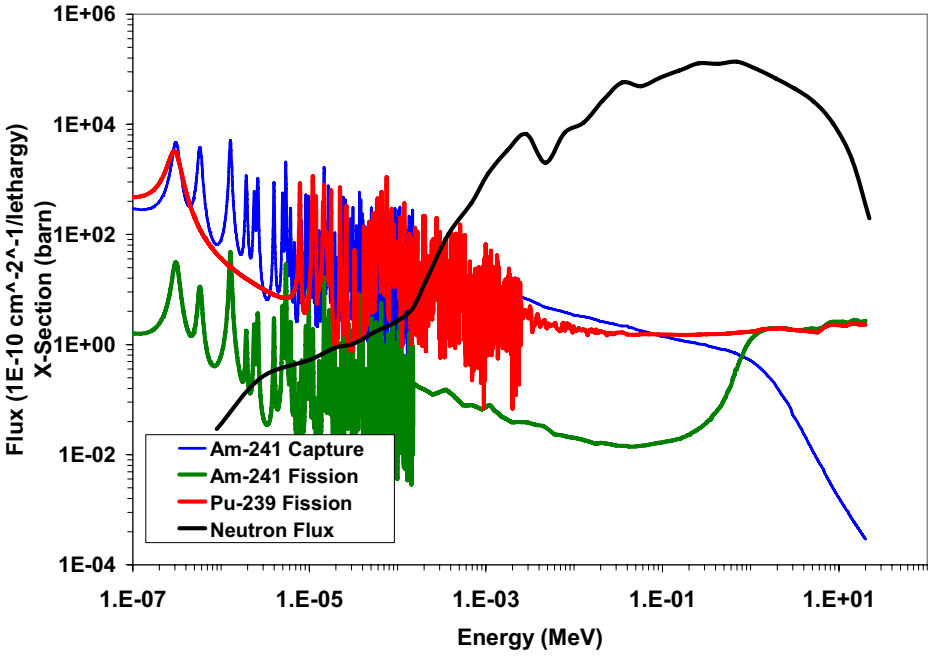

Figure 3: ENDF-VII Americium and Plutonium cross section plots versus SFR neutron spectrum

Because of the fission threshold, the Am-241 fission cross section below 1 MeV and above the resonance range (where the SFR neutron spectrum is very small) is two orders of magnitude less than for fission above 1 MeV (Figure 3). However, the capture cross section is almost as high as the Pu-239 fission cross section in the same energy range. Therefore, the HT-SFR target neutron spectrum is moderated slightly in order to reduce the neutron energy to just below 1 MeV. This increases the neutron capture in americium relative to plutonium fission in the targets. The effect can be seen by evaluating the ratio of total absorption in americium over total absorption in Pu-239. This increase can be observed by observing a capture and a fission based fuel utilization factor for the driver and the targets. In Table 2, a transmutation utilization factor is used to quantify the reaction probability of capture in a given isotope divided by any absorption in the region of space being studied. The transmutation utilization factor is defined in the equation below.

$$\text{transmutation utilization} = \frac{N_i \sigma_i^r}{\sum_i N_i \sigma_i^c + N_i \sigma_i^f}$$

Where: i represents a given isotope in targets or driver fuel and r represents capture or fission

Similarly, the fission utilization factor is defined as the reaction probability of fission in a given isotope divided by any absorption in the region of space being studied. Also supplied in Table 3 is a single group cross section ratio. The cross section ratio shows the spectral effect on the microscopic cross sections alone without being weighted by number density.

Table 2: Transmutation utilization factor

	Driver		Target	
	CAP/ABS	FISS/ABS	CAP/ABS	FISS/ABS
Am-241	1.59%	0.34%	15.64%	0.93%
Pu-239	6.02%	30.36%	8.24%	15.43%

Table 3: Single group cross section ratio

	Am-241CAP over Pu-239 FISS	Am-241 ABS over Pu-239 ABS
Driver	0.77	0.78
Target	1.33	0.91

It is important to note that the ratio of the Am-241 capture to the Pu-239 fission cross section is greater in the target than the driver fuel because of moderation. It is also apparent that the total absorption cross section ratio of Am-241 over Pu-239 is greater in the targets than the driver fuel because of this increased neutron capture. This effect explains how the capture utilization factor for Am-241 is nearly equivalent to the fission utilization in Pu-239 in the targets.

The slight target moderation results in a relatively epithermal flux compared to that for the active driver regions as shown in Figure 4. It is important to note that though the total flux in the targets is less than in the active driver, much of it is being depressed by resonance absorption. Much of the resonance absorption is in Pu-239 and U-238. However, resonance absorption in Pu-239 leading to fission serves to generate more neutrons. These neutrons have a relatively short mean free path because of the softer spectrum. Therefore, they remain within the target's neutron population. Moreover resonance absorption in U-238 serves to generate more Pu-239. The combination of epithermal spectrum and plutonium breeding by both Am-241 and U-238 creates enough plutonium to replace the initial plutonium loaded in the targets at beginning of cycle. As can be seen by Figure 5, the total amount of Pu-239 stays relatively

constant. The total plutonium content increases slightly, mainly from Pu-238,242 production from Am-241 transmutation.

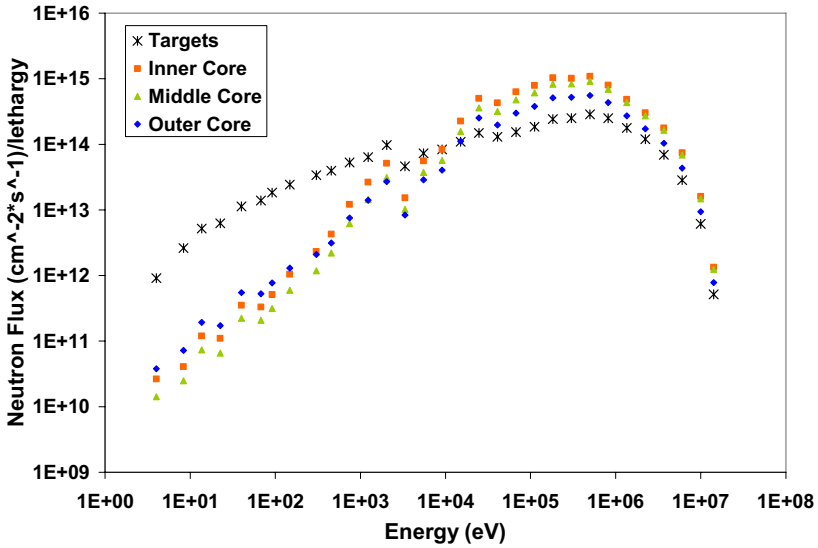

Figure 4: Target flux spectrum compared with the inner, middle and outer enrichment zone for a 101.6 cm tall HT-SFR with a pin-to-pitch diameter of 1.1.

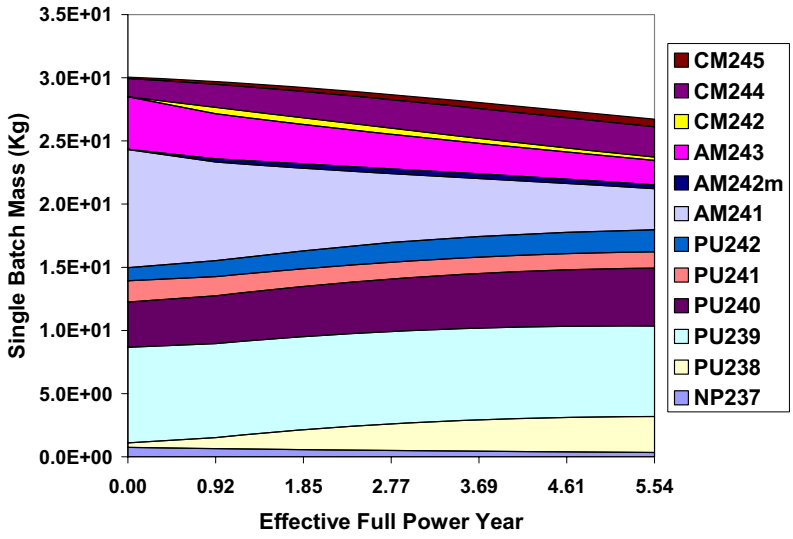

Figure 5: Change in isotope masses as a function irradiation time for the target region residing above the middle core (core height = 101.6 cm, p/d=1.1).

6. Parametric Study

Because the transmuted plutonium remains in the fuel cycle via the pyroprocessor, the amount of space reserved in the reactor for targets plays a significant role in the demand for the UREX+3 supplied Np&Pu. From a geometry standpoint, the ratio of target volume to core volume is dictated by the active core axial height. From a physics standpoint, the amount of Pu-239 breeding in the active core is a function of core flattening. Since, breeding excess Pu-239 in the active core is not a primary objective of

the HT-SFR, it is desirable to minimize the active core's conversion ratio. Conversely, since breeding even plutonium is an indicator of americium destruction, it is not necessary to minimize the target's conversion ratio.

The rate of americium destruction is a function of the target spectrum, active core axial leakage and target rod volume. As will be discussed in a later section, increasing the fuel rod diameter also increases the HT-SFR Am&Cm destruction rate. This is because increasing the target rod diameter also increases the amount of americium charged to the HT-SFR per cycle. If the reactor cycle is shortened, then the time rate of americium fed to the core is increased because the target mass loaded per cycle is constant. This does not, however, indicate the spectrum effect of the zirconium hydride content or flux intensity in the targets. Because the target irradiation time is not held constant, simply comparing the ratio of charged to discharged target americium is not an adequate indication of the destruction efficiency. Instead, a half-life is defined for Am-241 transmutation to quantify the magnitude of the capture reaction rate. This can be approximated using a first order differential equation because the rate of Am-241 production rate via beta decay from Pu-241 is relatively slower than the capture rate. Therefore, Am-241 destruction can be characterized with a purely exponential behavior just as with radioactive decay. This exponential behavior is given by the Am-241 production and decay rate equation.

$$\frac{dN}{dt} = \lambda_{Pu-241}^{decay} N - N\sigma_{Am-241}^{capture}\phi \Rightarrow \frac{dN}{dt} = \lambda_{Am-241}^{capture} N \Rightarrow T_{1/2}^{transmutation} = \frac{\ln(2)}{\lambda_{Am-241}^{capture}}$$

Table 4 shows the irradiation time required to reduce the americium mass by half.

Table 4: Transmutation Half-Lives (Years)

	p/d=1.1	1.176	1.293	1.357
101.6 cm	2.49	2.31	2.04	1.87
70.6 cm	2.73	2.54	2.24	2.06
50.6 cm	3.23	2.99	2.64	2.44

Notice the half-life decreases for decreasing pin diameter. This can be explained by the higher sodium fraction in the active core for decreasing fuel pin diameter. Increased leakage invests more neutrons in the targets. The decreasing half-lives with height are also related to axial leakage. However, the expected result is a decrease in half-life due to an increase in leakage with the core height reduction.

Because of the enhanced leakage, the driver fuel radial power profile develops a depressed region in the inner core with increased flattening. The increase in the americium transmutation half-life with decreasing core height is caused by a reduction in the intensity of neutrons leaving the inner core region. It is important to note the conformity of the three power profiles plotted in Figure 6 in the outer core area. This behavior is indicative of the cosine shape of the radial flux gradient as neutrons leave the core. The increased axial leakage shown in Figure 7 affects the curvature of the radial power profile in the inner core region more so than in the outer region. This is because the axial flux gradient is decreased more in the inner core than the outer core. The flux in the outer core regions are already suppressed everywhere by radial neutron escape. This explains the conformity of the three different radial power profiles in Figure 6 at the outer edge. The combined effect of a depressed radial profile and the decreased total reactor power for decreasing height also decreases the overall target and driver burnup. Because the power density becomes more evenly distributed axially and radially, the power density on the active core top surface becomes reduced. This is a sign of less power peaking. The reduction in power peaking in the inner core makes possible raising the reactor power for a given core height. Even though there is more axial leakage from the flattened design, there is also less flux in the targets. This reduction in flux is a result of the reduction in power for each reduction in core height. If the core power is increased such

that the maximum power density for the driver fuel is brought back to the limit given to the homogeneous reference core design, the target flux will be increased.

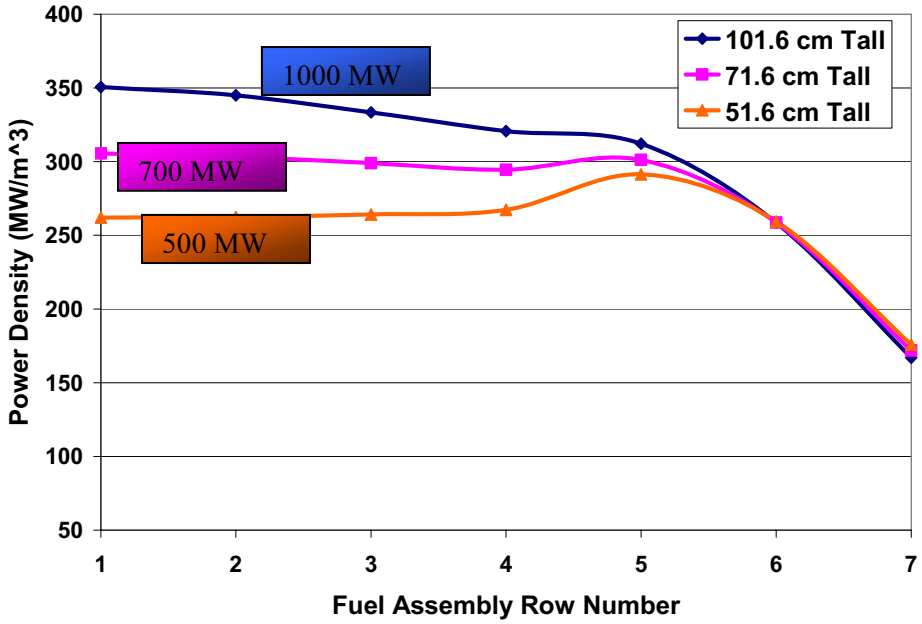

Figure 6: Active core radial power density profile for an HT-SFR with h_d: 101.6, 71.6 and 51.6 cm (p/d=1.1).

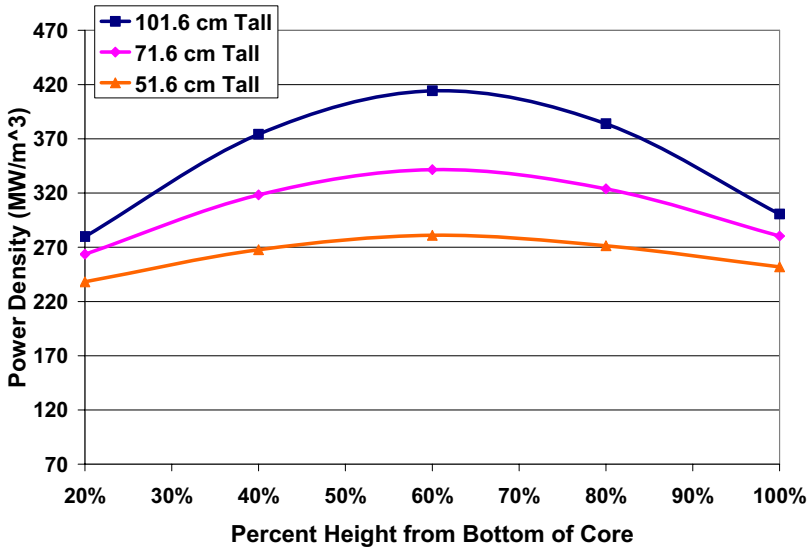

Figure 7: Inner core axial power density profile for an HT-SFR with h_d: 101.6, 71.6 and 51.6 cm (p/d=1.1).

The benefit of a smaller power gradient allows all fuel in the core, including the targets, to be irradiated at a higher power density with less peaking. After increasing reactor power, the higher power density in the targets translates into a higher flux density for transmutation. Therefore, the transmutation half-life for the targets of the flattened core with a more realistic power rating will be higher than for the parametric study where the power rating was reduced with reactor height.

The next section describes two flattened core geometries at a 1000 MW power level with a corrected radial power distribution to compare the target transmutation performance.

7. Tall and Flattened HT-SFR Options

Using the homogeneous core as a reference on equal fuel pin geometry, the HT-SFR height and pin design is varied. This was done to determine the combinations of core height and pin design that have an equivalent or enhanced reactor performance trait. The reactor performance traits considered were the excess reactivity, total core void worth and Doppler coefficient. The highest diameter fuel pin design (p/d=1.1) from Table 1 is selected to give a Doppler coefficient with increased negativity than the reference case. This is expected because the volume of fuel in the active core is increased and the percent of that fuel being uranium is also increased. After down-selection, the final active core geometry is 91.6 cm with a 1.1 pin pitch-to-diameter ratio. The 10 cm reduction in active core height was found to give a total core void worth that was slightly less than the homogeneous reference with the 1.1 pin pitch-to-diameter ratio. Though the active driver core height is 10 cm less than the homogeneous reference, the total core height is 10 cm "taller" due to the addition of the 20 cm length targets. This core design, as well as a much "flatter" core design, is compared to the homogeneous reference in Table 5. The flat HT-SFR core design, discussed next, is given in Figure 8.

Table 5: Core design summary for the homogeneous reference with tall and flat HT-SFR

	reference	tall	flat
Total Core Height	**101.6**	**110.6**	**91.6**
Active Driver Height	**101.6**	**91.6**	**71.6**
Total Core Volume (m3)	**3.3**	**3.6**	**4.0**
Active Core Volume (m3)	**3.3**	**3.0**	**3.1**
Rows of Driver Fuel	**7**	**7**	**8**
p/d	**1.1**	**1.1**	**1.1**
IC Enrichment	**14.92%**	**16.07%**	**18.65%**
Enrichment Split (IC/MC/OC)	**1.0/1.25/1.50**	**1.0/1.25/1.50**	**1.0/1.12/1.25**
Cycles per Enrich. Zone (IC/MC/OC)	**6/6/7**	**6/6/7**	**6/6/7**
Cycle Length (EFPD)	**322.86**	**319.90**	**350.58**

Because of its similarity in physical volume to the homogenous reference, the down-selected HT-SFR's power level is increased to 1000 MWth. This HT-SFR design (Figure 1, h_d=91.6,h_t=20 cm) represents a heterogeneous reactor with comparable reactor performance and safety attributes to the homogeneous reference (Figure 1, h_d=101.6,h_t=0 cm). For the flattened HT-SFR version, a 71.6 cm height is evaluated to observe a much larger target-to-driver volume ratio. An additional row of "outer core" drivers is added to this flat core so that the power density and total power is made comparable to the "tall" HT-SFR (Figure 8, h_d=71.6,h_t=20 cm). The enrichment splitting for this flat HT-SFR is modified to give a flattened radial power distribution similar to the 71.6 core from the parametric analysis.

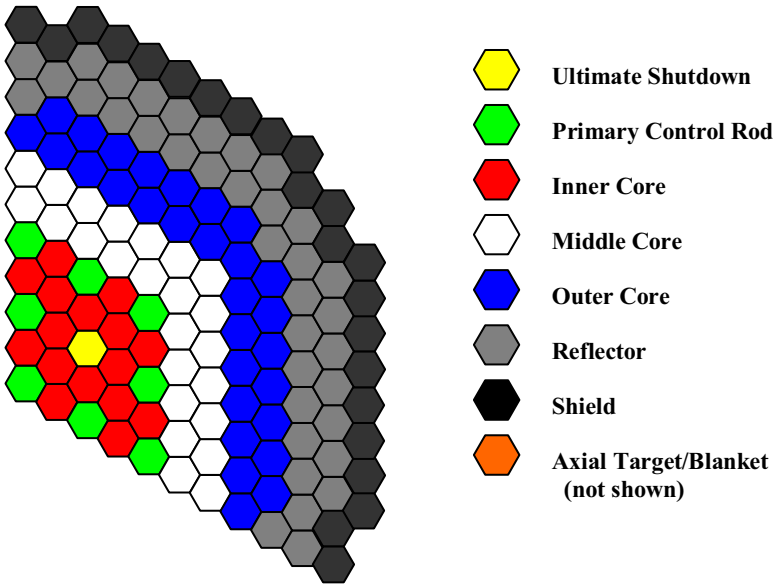

Figure 8: "Flat" HT-SFR (8 rows of fuel). The axial profile is given previously.

Because of the inherently flatter power distribution, the gradient of enrichment splitting for the flat HT-SFR can be decreased. Therefore, the "flat" core's middle and outer zones are enriched to 1.12 and 1.25 times that for the inner core respectively. This tailored enrichment splitting gives the flat HT-SFR a much flatter power distribution than the tall HT-SFR. The axial leakage works in parallel with the enrichment splitting to create an almost completely flat power profile across the inner and middle enrichment zone. Figure 9 shows the radial power distribution for six axial slices through the tall and flat versions of the HT-SFR. This initial estimation of the optimized enrichment splitting is sufficient to guarantee the highest power density in the inner core. Yet, it is apparent that the level of core flattening and the enrichment splitting could be varied independently until a true optimized power distribution is found.

Notice, the axial target power density is overall greater in the flat than the tall HT-SFR. The increased target power density is linked to the axial leakage from the active core. As seen in the transmutation half-life discussion, flattening the core reduces the axial and radial flux profile's curvature. This more shallow axial power profile provides a higher power density at the core axial periphery as seen in Figure 10. This increased power also provides for a reduced transmutation half-life of 2.22 years. Therefore, the Am&Cm destruction efficiency is actually comparable to the thin fuel pin design from Table 4. This higher efficiency combined with a larger overall target volume (more driver assemblies) gives a higher Am&Cm destruction rate when compared with the tall core. This higher Am&Cm destruction rate equates into a higher plutonium breeding rate. This increases the amount of Am&Cm and reduces the amount of Np&Pu drawn from the UREX+3 plant. Hence, the size of the surplus Np&Pu feed increases. In fact for both the tall and flat designs, the external Np&Pu feed for the active core is reduced to zero for the equilibrium fuel cycle. Consequently, the UREX+3 plant only needs enough Np&Pu to produce fresh targets.

For either case, the radial power profile falls off sharply in the outer two rows of fuel. This is attributed to the dominating radial leakage effect on the flux gradient in the outer core. It is important to note, the volume ratio of these outer two rows to the rest of the fuel is 0.5 and 0.44 for the flat and tall cores respectively. So the volume of target material located in the low flux of these outer two regions decreases as the core radius is increased. Hence, the flat HT-SFR has the smallest fraction of targets located above the low flux, low power driver fuel. This gives the flat HT-SFR the advantage of having the highest achievable transmutation rate over a greater share of the targets than the tall HT-SFR. So, the

average transmutation rate in the targets is highest for the flat core. In addition to the geometrical improvement in target exposure in the radial direction, the axial volume ratio of target to driver fuel increases with core flattening. This is because the target volume in the numerator of this ratio is fixed for a given radius by its 20 cm height, but the denominator is decreasing as the core height is decreasing. Therefore, the overall minor actinide charge rate per cycle increases as the active core height is decreased. The combined effect of increased axial leakage from the active core, increased share of high power rows of fuel and increase in minor actinide charge rate per cycle makes the flat HT-SFR design the most attractive transmutation system because of its physical ability to consume minor actinides.

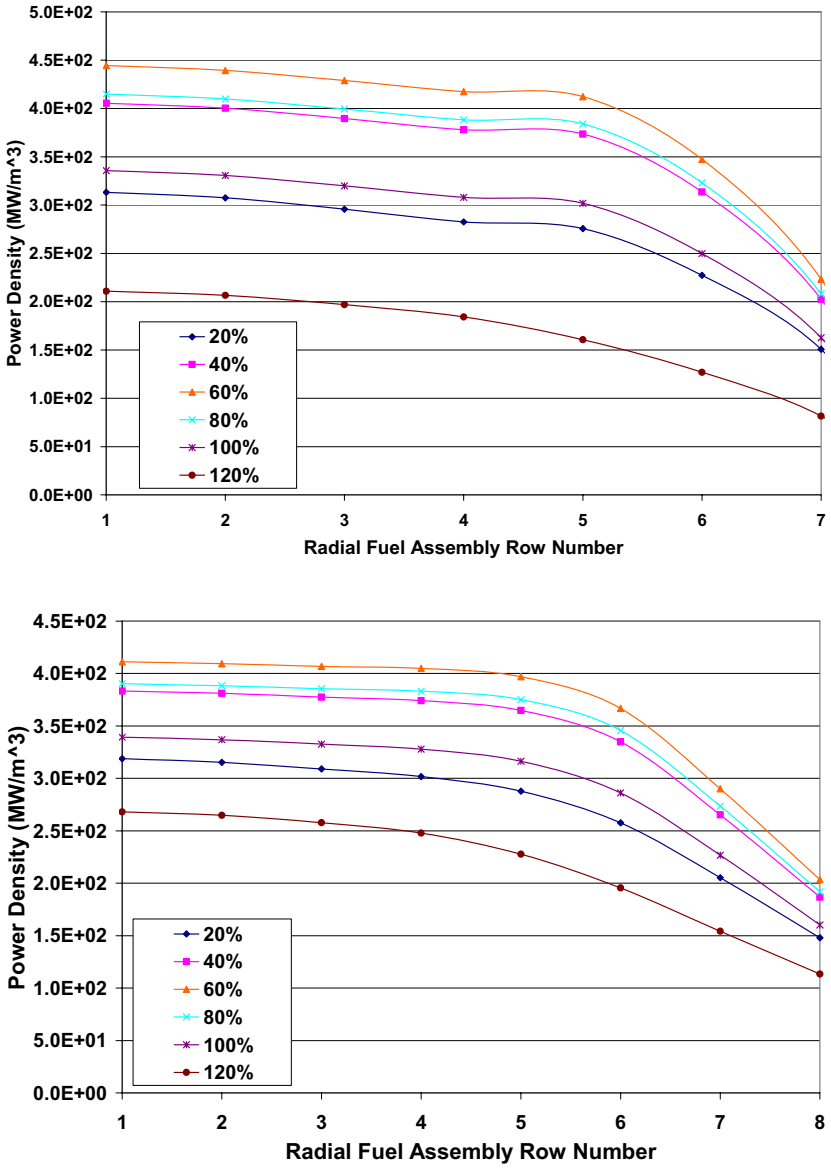

Figure 9: Radial power density profile for six axial slices through the core: Axial height is represented as a percentage of the full core height. (top = "tall", bottom= "flat")

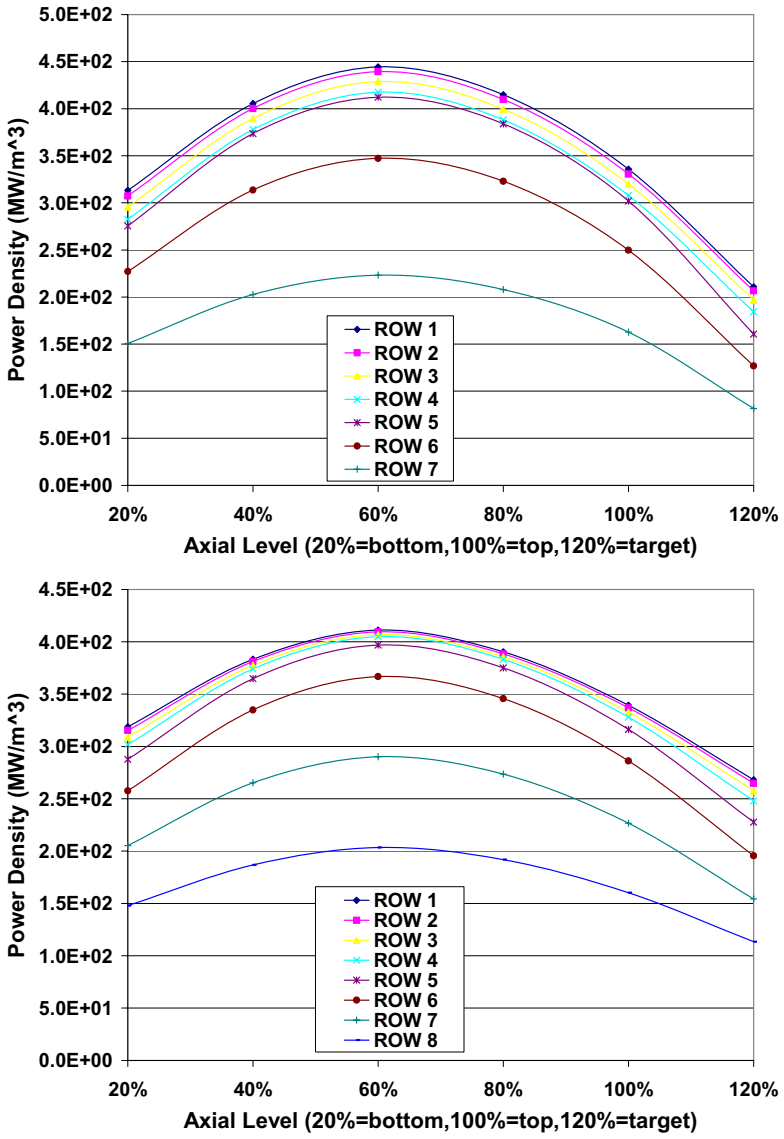

Figure 10: Axial power density profile for each row of fuel: Axial height is represented as a percentage of the full core height. (top = "tall", bottom= "flat")

Table 6 shows the fuel cycle parameters for the homogeneous reference compared to the tall and flat HT-SFR designs. As expected, the flat HT-SFR has a greater amount of Am&Cm being destroyed in the targets. This can be observed by examining the americium transmutation half-life for the flat verses the tall core design. In addition to a decreased transmutation half-life (increased capture reaction rate), the overall Am&Cm target destruction rate is also increased as can be seen in Table 6. The enhanced destruction rate is the combined effect of transmutation half-life and the target assembly charge rate.

Despite having a larger destruction rate in the targets the, the flat HT-SFR has a smaller overall Am&Cm consumption rate. This is because the flat HT-SFR has a longer cycle length (i.e.: refueling interval than the tall HT-SFR which is also equivalent to a smaller fresh target charge rate. Though the tall HT-SFR has a more efficient target (shorter transmutation half-life), these targets discharge a larger Am&Cm volume to the pyroprocessor. The tall core has a less efficient target but the shorter cycle length increases the rate that Am&Cm is charged to the targets and consequently the rate that un-transmuted minor actinide mass is received by the pyroprocessor. The difference in target destruction rate and total

core consumption rate illuminates the importance of distinguishing between the reaction rate of a given isotope and the actual charge rate of that isotope. The isotope destruction or reaction rate is a function of neutron flux and energy in any given region of the core, whereas the charge or consumption rate of a core design is more influenced by the mechanics of the fuel cycle operating at steady state.

In both cases, the amount of minor actinides diluted in the driver fuel is comparable to the reference and less than the 5% limit discussed earlier. The minor actinide percentage in the outer core is given in the Table 6 because the transuranic enrichment is the highest in that region because of the enrichment splitting. This driver fuel Am&Cm is effectively burned in the active core to the point where its quantity is not accumulating in the HT-SFR fuel cycle.

Table 6: Fuel cycle comparison for the homogeneous reference with tall and flat HT-SFR

	reference	tall	flat
Active Driver Height	**101.6**	**91.6**	**71.6**
Max MA in Driver Fuel			
OC Am/HM	**0.00%**	**1.72%**	**1.79%**
OC MA/HM	**1.06%**	**3.20%**	**3.40%**
TRU Externally Supplied Feed Rate			
Am&Cm Target Dest Rate (kg/EFPY)	**xx**	**1.48E+01**	**2.07E+01**
Am&Cm Feed Rate (kg/EFPY)	**2.79E+00**	**3.63E+01**	**3.31E+01**
Np&Pu Feed Rate (kg/EFPY)	**4.84E+01**	**3.60E+01**	**4.31E+01**
HM Feed Rate (kg/EFPY)	**3.75E+02**	**3.80E+02**	**3.75E+02**
Transmutation Half-Life			
IC Target Am Half-Life (Yr)	**--**	**2.49**	**2.22**

The Doppler coefficient and total core void worth are compared in Table 7. These performance parameters are calculated for core at the Beginning of Equilibrium Cycle using the calculation methods discussed earlier. This core design indicates that the Doppler coefficient decreases slightly from the active driver height reduction. This can be attributed to an increase in leakage and a reduction in parasitic capture as the active driver fuel height is reduced. An increase in axial leakage also decreases the positive void worth. This effect seems more related to total core height and not the height of the active driver fuel. However, when comparing the Doppler and void worth for each reactor type, there is little difference between safety performance indicators from case to case.

Conversion ratio is also sensitive to the leakage caused by core height reduction. The decrease in core height decreases the neutron capture probability and increases the fast escape probability.. The excess reactivity may be viewed in the same way. As leakage increases, the enrichment required to achieve the maximum fuel burnup of 18 atom percent also increases. This can be seen in Table 5. For the homogeneous case, this would normally reduce the cycle length because a reduction in U-238 capture also reduces the production of End of Equilibrium Cycle (EOEC) excess reactivity by Pu-239 formation. However, the flat HT-SFR design has the longest cycle length. This is attributed to the reactivity breeding effect of the axial target region. Since, the overall core size is larger for the flat verses the homogeneous or tall cases, there is actually less neutron escape when the targets are factored into the consideration. Therefore, neutrons are efficiently invested in excess reactivity recovery in the targets as the initial plutonium charge in the driver burns out.

Table 7: Physics performance comparison for the homogeneous reference with tall and flat HT-SFR

	reference	tall	flat
Active Driver Height	**101.6**	**91.6**	**71.6**
Total Core Void Worth (%)	**3.0502**	**3.1716**	**2.7975**
Doppler Coefficient (%/Kelvin)	**-4.491E-3**	**-4.677E-3**	**-4.218E-3**
Excess Reactivity (%)	**1.31**	**1.12**	**1.70**
BOEC k-eff	**1.01325**	**1.01312**	**1.01727**
Cycle Length (EFPD)	**322.86**	**319.90**	**350.58**
Max. Burnup (at.%)	**18%**	**18%**	**18%**
Dominance Ratio	**0.3798**	**0.3813**	**0.3958**
Conversion Ratio			
Core Conversion Ratio	**0.843**	**0.791**	**0.737**
Target Conversion Ratio	**--**	**0.714**	**0.705**
Inner Core Conversion Ratio	**1.00**	**0.954**	**0.847**
Middle Core Conversion Ratio	**0.793**	**0.748**	**0.733**
Outer Core Conversion Ratio	**0.679**	**0.638**	**0.663**

Also shown in Table 7 is the effect of total core size on the HT-SFR dominance ratio. The dominance ratio gives an indication of the closeness of the first and second lambda-mode eigenvalues. A larger dominance ratio (nearer to 1.0) is a measure of less neutronic coupling between the well separated regions of the core. Because the mean free path for fast neutrons is much larger than for thermal neutrons, sodium fast reactor fuel regions are normally well coupled, as confirmed by the very small dominance ratio's in Table 7. It is desirable to have a tightly coupled fast reactor from the standpoint of transient response. Since, the effective delayed neutron fraction for fast reactors is significantly less than for thermal systems; it becomes advantageous to reduce the complexity of the types of reactivity feedbacks that are expected to occur in the fast reactor. The flat HT-SFR has the largest total core volume compared to the other two designs and also has a moderated region (reduced mean free path). Nevertheless, the increase in dominance ratio is not significant compared to the homogeneous reference.

Table 8 evaluates the fuel performance indicators for the HT-SFR. One issue identified in previous heterogeneous target studies was that the transmutation of minor actinides into plutonium can create an undesirable power peaking effect. This issue was most pronounced for target irradiations in high flux regions in the inner core or for long "deep-burn" irradiations in the outer core. This work sought to diminish or eliminate the growth in target power from beginning-of-life (BOL) to end-of-life (EOL). For axial targets this is especially important because the targets share the same coolant channel flow orifice as the driver fuel. Sodium reactor fuel assemblies often are by and large designed with a metal shroud that encompasses the fuel pins. To keep a constant fuel temperature across the core, despite a large radial power gradient, sodium coolant flow in the channel is controlled on an assembly basis using an orifice at the bottom of the fuel assembly near where it meets the grid plate. If there were to be a wide change in target power, the amount of flow could be sufficient to cool the target at BOL and inadequate for EOL. Also, undesirable power peaking in the driver fuel could result if the power sharing between driver and targets shifts significantly throughout the irradiation.

Power peaking and shifting was minimized by choosing a target composition with a small amount of starting plutonium and uranium to ensure a slow net destruction of Pu-239 over the course of the irradiation. Also, the high importance of the Am-241 capture cross section in the epithermal flux ensured

that neutrons could be equally absorbed in americium as could be absorbed into Pu-239 (Table 2&3). This gives the americium the purpose of a burnable poison in the target as well as a fertile source for breeding even neutron number plutonium isotopes. These even neutron plutonium isotopes do not contribute significantly to the target fission rate because their fission importance is not high in that spectrum.

Table 8: Fuel performance comparison for the homogeneous reference with tall and flat HT-SFR

	reference	tall	flat
Active Driver Height	**101.6**	**91.6**	**71.6**
Linear Heat Generation Rate (kW/m)			
Peak Driver LHGR (kW/m)	**38.1**	**36.9**	**35.5**
Peak Target LHGR (kW/m)	**--**	**20.1**	**25.3**
Peak Fast Fluence: E>0.1 MeV (1E23 cm-2)			
Inner Core	**5.72**	**5.66**	**5.53**
Middle Core	**5.58**	**5.49**	**5.61**
Outer Core	**5.05**	**4.95**	**5.88**
Max Integral Fission Density: (f/cm^3)			
Driver Fission Density (1E21 f/cm3)	**6.96**	**7.67**	**7.09**
Target Fission Density (1E21 f/cm3)	**--**	**3.64**	**4.62**
Average Discharge Burnup (MWD/kg)	**124.4**	**127.3**	**134.1**

The peak Linear Heat Generation Rate (LHGR) in the targets was highest for the flat case. In all cases, the peak LHGR for the entire core occurred in the driver fuel not the targets. This peak driver LHGR occurs in the innermost row of fuel at the active core's mid-plane. This is also true of the volume and exposure integrated fission density for the target and driver fuel. Historically, the fission density has been used as an indicator of irradiation induced swelling and gas release in metal fuels. It allows equal comparison of fuel performance when the amount of heavy metal loading is not constant in the comparison. This is the case for the HT-SFR because the metal driver fuel and targets have different zirconium contents in their alloying. For all cases the peak fission density is less in the targets than it is in the fuel. Hence, the expected swelling and gas release, including transmutation helium, should be similar to that of past experience with metal driver fuel for equivalent fission density. This assumes that the rate of void formation and interconnected porosity in the target is roughly equivalent for the lower zirconium content driver alloy.

In addition, the smaller radial power density gradient for the flat case gives its driver fuels the smallest peak LHGR. The flatter power profile also explains the higher peak fast fluence in the outer core for the flat case than the other core designs. Notice the peak fluence limit for all the core designs mentioned is not constrained to the 4E23 cm^{-2} limit for HT-9 discussed earlier. However, it is noteworthy that a more evenly distributed fast flux also results in a more level fast flux exposure between the inner, middle and outer core regions. Similar to LHGR, this allows more of the fuel to be irradiated to a level closer to the $4x10^{23}$ cm^{-2} limit. As discussed in the "Calculation Method" section, the constraining parameter on the fuel cycle was the peak fuel burnup at the midpoint of the first row of fuel. The next section discusses a final down selection that reduces the cycle length such that the technical irradiation damage limits for the HT-9 structural components are met.

8. Fuel Cycle Aspects of HT-SFR

A final down selection in HT-SFR core design is made based on the transmutation and reactor physics attributes of the flattened case. The pin diameter of the flat design from above is reduced to increase enrichment in order to give a shorter cycle length. The shorter cycle length gives an acceptable fluence and displacement per atom (dpa) in the HT-9 structural materials. The only parameter changed in the fuel assembly design is an increase in the pin pitch-to-diameter ratio from 1.1 to 1.176. The resulting pin diameter is equal to the ABR CR=0.75 design and also closely matches the S-PRISM driver fuel pin dimension. The slight increase in enrichment also had the benefit of decreasing the HT-SFR conversion ration. Due to the poor transmutation performance of the targets residing in the outer core assemblies (row 7 and 8), they were consequently removed. The removal of these targets resulted in a higher plutonium quality to the overall target mass sent to pyroprocessing.

A comparison is made between this reduced enrichment and conversion ratio flat HT-SFR with the homogeneous metal ABR CR=0.5 design. It was the lateral core layout of this ABR design that became the basis for the homogeneous reference cases used for comparative analysis of the above parametric study. Therefore, this core shares the lateral core layout and fuel design described in the top half of Figure 1. Also, the pin pitch-to-diameter ratio for this design is 1.293 and the number of fuel pins is 324. Because of the significant change in fuel pin size and assembly design, this design is somewhat more exotic than the fuel designs used in past reactor designs such as FFTF and S-PRISM [13]. This is why the HT-SFR fuel assembly design is based on the metal ABR CR=0.75 instead of the CR=0.5 design. Table 9 gives a comparison of various reactor and fuel cycle attributes of both flat HT-SFR compared with a homogeneous ABR with CR=0.5.

Table 9: Reduced conversion ratio and cycle length ABR and HT-SFR.

	ABR CR=0.5	**HT-SFR CR=0.7**
Total Core Height	**101.6**	**91.6**
Active Driver Height	**101.6**	**71.6**
p/d	**1.293**	**1.176**
Calculated Conversion Ratio	**0.53**	**0.718**
IC Enrichment	**26.6**	**20.77%**
Excess Reactivity	**2.85%**	**1.23%**
Delayed Neutron Fraction	**0.00350**	**0.00333**
Cycle Length (EFPD)	**219**	**214**
Peak Fast Fluence: E>0.1 MeV (1E23 cm^{-2})		
IC: Row 1 - Midplane	**4.00**	**3.55**
Displacements per Atom in HT9 (dpa)		
IC: Row 1 – Midplane	**182.7**	**160.4**

Since the overall conversion ratio is higher for the HT-SFR, it is expected that the transuranic enrichment is smaller than the HT-SFR. The HT-SFR's transuranic enrichment is just inside the current experience database with Pu-U-Zr fuel alloys tested in fast reactors in the 1980's [14-15]. Also because of the smaller enrichment, the excess reactivity for the HT-SFR is less than the ABR. The selection of the pin pitch-to-diameter ratio was not optimized to make the fluence and dpa limit as close to the $4x10^{23}$ cm^{-2}

and 200 dpa limits as possible. Instead, it was statically selected on the basis of most probable and feasible fuel composition and assembly design. Extending the cycle length is possible by decreasing the driver fuel enrichment but results in an increasing conversion ratio due to increased parasitic capture.

Table 10 shows the rate of minor actinide and plutonium consumption. The HT-SFR burns less total TRU than the ABR but roughly twice the amount of minor actinides. Also the HT-SFR burns almost as many minor actinides as it does plutonium. For comparison Table 10 also shows the amount of material produced for a typical Generation II Pressurized Water Reactor (PWR) fueled with enriched Uranium Oxide (UOX) fuel burned to 51 MWD/kg. Also shown is the amount of plutonium consumed and minor actinides produced in a Generation III Evolutionary Pressure Reactor (EPR) filled with a full core of Mixed Oxide (MOX) fuel. This MOX fuel was given a 10 w/o plutonium enrichment and burned to 51 MWD/kg. The theoretical two-tier fuel cycle from Figure 2 is approximated by constructing a set of linear equations that represent the mass balance of materials produced or destroyed between the PWR, EPR and HT-SFR or ABR from Table 10.

Table 10: Mass production and destruction rates per installed megawatt per year.

	ABR CR=.5	**HT-SFR**
Total Core Height	**101.6**	**91.6**
Pu Consumption (kg/MWY)	**0.1564**	**0.0519**
MA Consumption (kg/MWY)	**0.0174**	**0.0400**
	UOX PWR	**MOX EPR**
Pu Consumption (kg/MWY)	**-0.0758**	**0.2033**
MA Consumption (kg/MWY)	**-0.0074**	**-0.0482**

$$M_{Pu}^{PWR} \times x_{PWR} - M_{Pu}^{EPR} \times x_{EPR} - M_{Pu}^{HTSFR} \times x_{HTSFR} = 0$$

$$M_{MA}^{PWR} \times x_{PWR} + M_{MA}^{EPR} \times x_{EPR} - M_{MA}^{HTSFR} \times x_{HTSFR} = 0$$

Where: M represents the coefficients in Table 10 and x represents the amount of installed thermal power capacity for a given reactor type.

Solving the above equations results in a fuel cycle having two MWth of installed HT-SFR thermal power per one MWth of EPR to burn all the transuranics produced by four MWth of PWR. By comparison, the ABR CR=0.5 would require two MWth to destroy the transuranics produced in four PWRs. However, this requires a more exotic fuel composition and fuel assembly design than the HT-SFR driver. If the fuel design and core layout of the metal ABR CR=0.75 is used, the ratio of ABR installed power to PWR installed power is near unity. Therefore, it is apparent that the number of HT-SFR's needed to close the fuel cycle with PWR's in the two tier scenario is about equal to the ABR CR=0.5 single tier scenario. In addition, the fuel composition and fuel assembly design can be kept closer to the ABR CR=0.75 reactor which has technical feasibility advantages over the ABR CR=0.5 core.

9. Conclusions and Future Work

Earlier studies indicate that a low conversion ratio SFR is necessary to destroy the undesired transuranics waste isotopes found in SNF. From a physics standpoint a low conversion ratio is ideal for reducing the production of plutonium and minor actinides by reducing parasitic capture in uranium. This work makes a fundamental change in philosophy regarding minor actinide waste management. Previous repository studies recognize the Am-241 concentration within transuranic waste as the most limiting isotope for the SNF amount that can be stored in a geologic repository. Because this isotope is not fissile, its removal from the fuel cycle is best achieved by parasitic capture. Because parasitic capture in americium leads to a transmutation path ending in even mass number plutonium isotopes with high fast fission worth, it can be used as a fertile blanket material.

Parametric studies were performed on a SFR with slightly moderated americium targets in an axial blanket. This HT-SFR parametric analysis revealed that high americium destruction in axial targets is achievable by flattening the active driver core. Recovering neutron in the targets allows the active core to have a high axial neutron leakage which enhances void performance and reduces active core conversion ratio. Because the fuel cycle goal is redefined for optimized destruction of americium instead of plutonium, a low conversion ratio is not the primary objective of the design. This reduces the need for smaller diameter fuel pins and their associated high enrichment and reactivity swing. However because some of the americium content discharged from the targets is incorporated into the driver fuel, some height reduction is necessary to ensure a void coefficient comparable with an equivalent homogeneous design. This conclusion was made evident by comparing the tall version of the HT-SFR. The tall HT-SFR required only a 10 cm height reduction to have a void coefficient comparable with the homogeneous reference.

Reducing the core height decreases the curvature of the axial power profile by increasing the axial leakage. This axial leakage places more flux in the axial targets for decreasing core height. Increasing the axial flux also increases the target transmutation rate. This reduces the Am-241 transmutation half-life. The transmutation half-life is used as an indicator of the americium destruction efficiency because it is a direct reflection of the flux and neutron spectrum in which the targets are exposed. It was also found that if the height is made sufficiently small, the radial power profile of the inner and middle core can be flattened by axial leakage. For the flat version of the HT-SFR, this effect resulted in a lesser degree of enrichment splitting, less power peaking in the driver fuel and a higher overall transmutation rate in the targets. The more evenly distributed power and flux distribution also decreases the relative difference between the peak fast fluence exposure experienced by the inner, middle and outer core regions.

This flat case had a smaller transmutation half-life than the taller core. The flat core's target volume was increased by adding an eighth row of fuel assemblies. The combination of these effects allowed the flat reactor to have a higher reprocessing feedback of target bred plutonium in the fresh charge of driver fuel. The efficient transmutation of americium into even isotope plutonium allows for high minor actinide destruction rate. The high americium consumption rate relative to plutonium creates a plutonium surplus at the aqueous plant where the SNF is originally separated. This surplus SNF reactor grade plutonium may be adequately burned in Generation III reactors fueled with MOX.

Since LWR MOX can have a conversion ratio varying in the range of 0.6 to 0.8, by definition it has a comparable percentage of TRU destruction to TRU production to the HT-SFR or ABR. However, LWR MOX is not ideally suitable for minor actinide transmutation due to the complexities that minor actinides bring to the fuel design. These issues are related to fuel fabrication, fuel irradiation performance and fuel handling associated with high radiation fields. All of these effects combined create a fuel cost uncertainty

that is assumed for this work to be not tolerable in the commercial LWR industry. In contrast, SFRs are designed to have a high tolerance for fuel degradation in the reactor as well as high radiation fields. SFR technologies have previously been demonstrated with relative certainty to work well with dedicated and co-located "hot" fuel repossessing and fabrication facilities. Because of the lack of interim storage for fission product cooling for many SFR fuel cycles, the turnaround time for fuel discharge to refueling is generally short. Therefore, "hot" fuel handling implies working with fuels that are still physically and radioactively hot. Thus, these types of dedicated fuel cycle facilities are assumed for this work to be more suitable for handling the exotic nature of minor actinide transmutation than the LWR infrastructure.

This work demonstrates the axial heterogeneous reactor potential of mitigating the closed fuel cycle feasibility uncertainty by minimizing the amount of dedicated SFRs needed to destroy the SNF created by LWR UOX fuel. This is achieved by a high minor actinide consumption rate in the SFR component of the overall fuel cycle. A very simplistic calculation to represent the mass balance between SFRs and LWRs was devised to demonstrate this point. It was found that the number of sodium fast reactors needed to support the LWR fuel cycle component can be reduced by roughly half if the heterogeneous reactor design is employed.

10. References

1. Morris, E., Smith, M. (2002) Development of Low Conversion Ratio Fast Reactors for Transmutation, Argonne National Laboratory, ANL-AAA-057

2. Choi, H., Downar, T. (1999), A Liquid-Metal Reactor for Burning Actinides of Spent Light Water Reactor Fuel-I: Neutronics Design Study, Nuclear Science and Engineering, 133, 1-22, Sept. 1999

3. Hoffman, E., Yang, W., Hill, R. (2006) Preliminary Core Design Studies for the Advanced Burner Reactor Over a Wide Range of Conversion Ratios, Argonne National Laboratory, ANL-AFCI-177

4. Moore, K., Young, W., (1968), Phase Studies of the Zr-H System at High Hydrogen Concentrations, Journal of Nuclear Materials, 27, 316-324, September 1968

5. Stanculescu, A., Garnier, J., Rouault, J., Kiefhaber, E., Sunderland, R., (1994), Plutonium Burning and Actinide Transmutation in Fast Reactors: First Results Obtained within the Frame of the CAPRA Programme, International Nuclear Congress Atoms for Energy (ENC '94), 2, 558-565, Lyon, France, October 2-6, 1994

6. Wade, D., Hill, R., (1997), The Design Rationale of the IFR, Progress in Nuclear Energy, 31, 1-2, 13-42, 1997

7. Hill, R., Wade, D., Liaw, J., Fujita, E., (1995), Physics Studies of Weapons Plutonium Disposition in the Integral Fast Reactor Closed Fuel Cycle, Nuclear Science and Engineering, 121, 17-31, Sept. 1995

8. Hilton, B., Hayes, S., Chang, G., (2006), Irradiation Performance of Fertile-Free Metallic Alloys for Actinide Transmutation, Proceedings of the 11th Workshop on the Research, Deployment and Implementation of Fissile-Free Nuclear Fuels, Park City, UT, October 10-12, 2006

9. Toppel, B. (1983), A User's Guide to the REBUS-3 Fuel Cycle Analysis Capability, Argonne National Laboratory, ANL-83-2

10. Henryson, H., Toppel, B., Stenberg, C., (1976), MC2-2: A Code to Calculate Fast Neutron Spectra and Multigroup Cross Sections, ANL-8144

11. Derstine, K., (1984), DIF3D: A Code to Solve One-, Two-, and Three-Dimensional Finite-Difference Diffusion Theory Problems, ANL-82-64

12. Wigeland, R. A., Bauer, T. H., (2004) Repository Benefits of AFCI Options, Argonne National Laboratory, ANL-AFCI-129, September 2004

13. A. E. Dubberley, K. Yoshida, C. E. Boarman, and T. Wu, "SuperPRISM Oxide and Metal Fuel Cre Designs," Proceedings of ICONE 8, 8th International Conference on Nuclear Engineering (2000).

14. C. E. Lahm, J. F. Koenig, R. G. Pahl, D. L. Porter, and D. C. Crawford, “Experience with Advanced Driver Fuels in EBR-II,” Journal of Nuclear Materials, 204, 119 (1993).

15. A. L. Pinter and R. B. Baker, “Metal Fuel Test Program in the FFTF,” Journal of Nuclear Materials, 204, 124 (1993).